Strain and retrogression partitioning explain long-term stability of crustal roots in stable continents

Bénédicte Cenki-Tok, P. F. Rey, D. Arcay

Publisher: GSA
Journal: GEOL: Geology
DOI:10.1130/G47301.1

[1]GSA Data Repository item 2020xxx, Table DR1 (thermal and mechanical parameters), Figure DR1 (slow modeling results), Figure DR2 (fast modeling results), and the Python input file (Script-G47301_285-Cenki-Tok-etal.ipynb), is available online at http://www.geosociety.org/datarepository/2020/, or on request from editing@geosociety.org.

Strain and retrogression partitioning explain long-term stability of crustal roots in stable continents

B. Cenki-Tok[1,2]*, P.F. Rey[2] and D. Arcay[1]

[1]*Géosciences Montpellier, Université de Montpellier, CNRS, 34095 Montpellier cedex 5, France*

[2]*Earthbyte Research Group, ARC ITRH Basin GENESIS Hub, School of Geosciences, University of Sydney, Sydney, New South Wales 2006, Australia*

*E-mail: benedicte.cenki-tok@umontpellier.fr

ABSTRACT

Away from tectonically active regions, the continental crust has an average thickness of 40 ± 1 km. Yet, it shows a remarkable variability from 25 to 65 km, comparable to that of the most tectonically active regions. Here, we consider the problem of the formation and preservation of anomalous deep crustal roots in stable intracontinental regions. Using two-dimensional thermomechanical experiments, we show that the interplay between partial melting, the formation of garnet-pyroxene-bearing rocks, and their strain rate–dependent retrogression result in the preservation of thick and strong crustal roots. We argue that it is the partitioning into narrow regions of strain, retrogression, and weakening coupled into a positive feedback loop that explains why

strong high-grade crustal roots remain largely immune to gravitational stresses and are able to persist over hundreds of millions of years.

INTRODUCTION

The crust-mantle transition is generally well-defined on geophysical images, enabling detailed knowledge of crustal thickness at global and regional scales (Prodehl et al., 2013). Discarding tectonically active regions, the thickness of the stable continental crust has a global average of ~40 km (±1 km error on the calculated average crustal thickness) (Christensen and Mooney, 1995; Fig. 1A). Yet, crustal root anomalies as much as 65 km deep exist in all stable continents (e.g., Szwillus et al., 2019) from cratonic regions such as the Baltic and Canadian Shields (Cook et al. 2010; Artemieva and Thybo, 2013; Fig. 1B) to Proterozoic and Paleozoic terranes such as Antarctica and Australia (Salmon et al., 2012; An et al., 2015; Ebbing et al., 2018; Fig. 1C). Some of these crustal roots have been interpreted as inherited regions of thick orogenic crust (e.g., Fischer, 2002; Studinger et al., 2004), others as mantle-derived mafic roots accreted below a continental crust of normal thickness (e.g., Thybo and Artemieva, 2013). In both cases, we expect that the enhanced heat flow would thermally weaken the deep crust, enabling efficient viscous flow to relax gradients of crustal thickness and to flatten the Moho on a regional scale (Clark and Royden, 2000; Beaumont et al., 2001; Nábělek et al., 2009; Rey et al., 2010). Hence, the persistence over hundreds of millions of years of thick crustal roots poses an intriguing problem. Although high heat flow produces migmatites and granites that contribute to the transient weakening of the deep continental crust, it also produces drier and stronger garnet-pyroxene rocks such as granulites (e.g., Jackson et al., 2004). Upon cooling, hydration, and deformation, these stronger rocks may be retromorphosed into weaker amphibolitic gneisses. Here, we explore through two-dimensional (2-D) thermomechanical experiments how the interplay between mechanical weakening due to partial melting, strengthening and density increase due to the crystallization of garnet-pyroxene assemblages, and post-orogenic weakening due to retrogression may impact the long-term crustal thickness. Our results suggest that thick crustal root anomalies could be the remnants of dry garnet-pyroxene-bearing rocks that survived post-orogenic extension and retrogression. These garnet-pyroxene-bearing crustal-scale boudins strengthen the lower crust and reduce its capacity to flow. Our experiments are a first step toward explaining why relaxed orogenic crust may maintain heterogeneities in crustal thickness hundreds of millions of years after orogeny has ceased.

NUMERICAL EXPERIMENTS, CODE, AND MODEL SETUP

Our 2-D thermomechanical experiments consider a 360-km-wide orogenic plateau with a 70-km-thick crust (i.e., the thickness of the Tibetan Plateau; Nábělek et al., 2009) above 40 km of mantle (Fig. 2). A layer of air-like material with low viscosity and low density is imposed on top of the crust to accommodate the development of surface topography. The plateau experiences extensional deformation as the crust returns to a normal thermomechanical state. Extensional-velocity boundary conditions are imposed on both vertical walls of the model. We have tested slow (0.18 cm yr^{-1}) and fast (1.8 cm yr^{-1}) velocities, delivering a strain rate averaged over the length of the model of 3×10^{-16} s^{-1} and 3×10^{-15} s^{-1} respectively. Horizontal boundaries of the model are free slips. The thermal properties of the material combined with constant basal heat flow and constant top temperature deliver an initial steady-state geotherm leading to a Moho temperature of

Publisher: GSA
Journal: GEOL: Geology
DOI:10.1130/G47301.1

~900 °C (Fig. 2). We select from the literature plausible visco-plastic parameters (see the GSA Data Repository[1]) so the mechanical behavior of the modeled lithosphere depends on temperature, strain rate, deviatoric stress, and accumulated strain. Details of modeling procedures, rheological and thermal parameters, as well as the input Python script are available in the Data Repository.

In order to explore the interplay between partial melting, the formation of stronger garnet-pyroxene-bearing rocks, and their retrogression into weaker amphibolite facies rocks, we parameterize three first-order metamorphic phase transitions. The first phase change simulates partial melting and its feedback on density, viscosity, and temperature (Rey et al., 2009; see the Data Repository). A second phase change with feedback on density and viscosity occurs at temperature $T = 777$ °C to simulate prograde amphibolite to garnet-pyroxene rock reaction (Philpotts and Ague, 2009). Finally, a third phase change with feedback on density and viscosity accounts for the retrogression of garnet-pyroxene-bearing rocks back into amphibolite facies rocks. This third phase change occurs at $T = 777$ °C as well and for a strain rate $\geq 10^{-14}$ s^{-1}. Our model implicitly assumes that water is available. Therefore, retrogression is contingent upon strain rate, which simulates the metastability of dry high-grade rocks during exhumation. This strain-rate threshold is in the range of expected strain rates measured in orogenic shear zones (Sassier et al., 2009; Boutonnet et al., 2013; Fagereng and Biggs, 2019). Rock solidus depends on rock fertility and availability of fluid. Hence, we have tested different solidii for the continental crust and the garnet-pyroxene-bearing rocks (Data Repository) in the range commonly accepted for these rock types. For the continental crust, we have tested a solidus representative of fertile metapelites with a melting temperature at room pressure of 650 °C (Figs. 3A and 3B; White et al., 2001), and a solidus representative of less-fertile rocks with a melting temperature at room pressure of 720 °C (Fig. 3C; Rey and Müller, 2010). For the dry garnet-pyroxene-bearing crust, we use a melting temperature at room pressure of 790 °C representative of refractory granulites (Cenki-Tok et al., 2016). We use *Underworld,* a well-tested open-source finite-element code (https://underworld2.readthedocs.io/), to solve the equations of conservation of momentum, mass, and energy for an incompressible fluid on a Cartesian Eulerian mesh (Moresi et al., 2007; Beucher et al., 2019).

RESULTS

When a slow divergent velocity is imposed (0.18 cm yr^{-1}), the crust thins homogeneously, the Moho remains flat, and deformation is dominated by pure shear strain whether melt and/or garnet-pyroxene rocks are present or not (Fig. DR1 in the Data Repository). In contrast, under faster extensional velocities (1.8 cm yr^{-1}), the experimental outcome depends on phase changes. When the formation of strong garnet-pyroxene rocks is not allowed, partial melting makes the deep crust hot and mobile, which allows the formation of a migmatitic dome (Fig. 3A). In the partially molten dome, finite strain ellipses are strongly flattened, with a vertical long axis indicating the presence of a vertical high-strain zone separating two sub-domes. This double-dome geometry has been well documented (Rey et al., 2011, 2017; Korchinski et al., 2018). Figures 3B and 3C show a different result when prograde garnet-pyroxene rock formation and retrogression into amphibolite are allowed. In the case where retrogression does not occur (Fig. DR2A), the crust thins homogeneously. As the formation of garnet-pyroxene rocks strengthens the deep crust, its capacity to flow is much reduced and the upper crust remains mechanically coupled to the mantle. Extensional deformation is more distributed and heterogeneous as documented by the crustal-scale pinch-and-swell strain pattern, as well as the finite strain field imaged by the finite strain ellipses (Fig. 3B). As strain rate controls the retrogression of garnet-pyroxene rocks (Figs. DR2B and DR2C), we observe that retrogression is partitioned into the pinch regions where strain rate is higher, whereas garnet-pyroxene pods are preferentially preserved in the swell regions where strain rate is lower and below the threshold required to activate retrogression. Because retrogression leads to weakening, favoring strain localization and therefore higher strain rates, there is a positive feedback loop between strain rate, retrogression, and weakening. When the crustal solidus is that of a fertile metapelite, portions of the lower crust are partially molten and able to flow under gravitational stresses, whereas flow is inhibited in the strong garnet-pyroxene rock pods (Fig. 3D). Raising the solidus temperature of the continental crust by 70 °C results in a similar outcome except that there are no more partially molten domains within the continental crust (Fig. 3C). Because of the formation of garnet-pyroxene rock pods, the Moho presents a winding geometry with crustal thickness variations of as much as 50%, from 35 to 53 km. After 25% of extension and thinning, we have left these experiments to thermally and mechanically relax over 180 m.y. under fixed boundary conditions (i.e., setting the kinematic boundary condition to 0 cm yr^{-1}). We observe that the heterogeneity of crustal thickness persists throughout this long cooling history.

DISCUSSION

Our numerical experiments suggest that strain rate–dependent retrogression that typically localizes along ductile shear zones cutting through high-grade rocks may

Publisher: GSA
Journal: GEOL: Geology
DOI:10.1130/G47301.1

explain how remnants of thick and strong orogenic crust can survive orogenic collapse. These regions can be ~50% thicker than the adjacent crust and as narrow as a few tens of kilometers across, and survive for hundreds of millions of years. Anomalous deep crustal roots have been imaged in stable intracontinental regions all around the globe. In the eastern Canadian Shield, for example, the Lithoprobe project (https://lithoprobe.eos.ubc.ca/) has documented several crustal roots (Cook et al., 2010). Below the Torngat orogen along the eastern Canadian Shield, a Paleoproterozoic crustal root as much as 50 km deep, 15 km deeper that the average adjacent crust, and ~80 km wide and >200 km long has been imaged on seismic profiles (Fig. 1B; Funck and Louden, 1999). It is interesting to note that this Paleoproterozoic crustal root is bounded to the north and east by major shear zones (Cook et al., 2010). In the Baltic Shield, along an Archean–Paleoproterozoic suture, the Moho reaches a depth of ~60 km over a region centered on southern Finland (Artemieva and Thybo, 2013). In central Australia, even though this continent has been tectonically relatively stable for the past 300 m.y., crustal roots reaching 65 km depth have been imaged as deep regions of diffuse reflectivity over circular domains a few hundred kilometers in diameter (Fig. 1C; Kennett et al., 2011; Salmon et al., 2012). In Antarctica, a series of crustal roots as much as 60 km deep have been documented between Dronning Maud Land and Gamburtsev Subglacial Mountains (An et al., 2015; Ebbing et al., 2018). In peninsular India, made up of Archean to Paleozoic terranes, the Moho depth varies from ~38 km below the southernmost tip of India’s Proterozoic Southern Granulite terrane, to 50 km below the Archean Dharwar craton in semicircular regions ~250 km in diameter (Reddy and Vijaya Rao, 2013; Das et al., 2019). The structure and nature of the lower crust below the Southern Granulite terrane is heterogeneous, but because the middle and upper crust shows a constant thickness of 20–25 km, this variability must be accommodated by variation in thickness of the lower crust (18–32 km; Das et al., 2019).

The gravimetric and seismic characteristics of these crustal roots suggest the presence of garnet-pyroxene-bearing rocks. For example, in Canada, crustal roots showing P-wave velocities >7 km s^{-1} led Cook et al. (2010) to propose that in the absence of later tectonic reworking, the variations in Moho depth originate solely from rheological variations. In southern India, crustal roots display compressional-wave velocities that are systematically >7 km s^{-1} (Reddy and Vijaya Rao, 2013), and shear-wave velocities between 4 and 4.2 km s^{-1} (Das et al., 2019). The contrasting density and seismic characteristics between granitic rocks and/or amphibolite facies gneisses (<2700 kg m^{-3} and <6.4 km s^{-1}) and higher-grade garnet-pyroxene-bearing rocks (>2800 kg m^{-3} and >6.6 km s^{-1}; Christensen and Mooney, 1995; Artemieva and Thybo, 2013) suggest that deep crustal roots are made of the latter (Williams et al., 2014). This proposition is compatible with the seismically diffuse boundary that is commonly observed between the lower crust and the mantle (O'Reilly and Griffin, 2013). Because the petrophysical properties of garnet-pyroxene-bearing rocks are intermediate between the ones of the crust and the mantle, a garnet-pyroxene-rich lower crust would explain the seismic properties of the transition between the crust and the mantle observed in Peninsular India for example (Reddy and Vijaya Rao, 2013).

Importantly, in all of these examples, crustal roots are interpreted as inherited remnants of ancient orogenic crust that have survived gravitational collapse and the flattening of the Moho. We propose that these strong orogenic crustal roots owe their survival to the presence of retrogressed and therefore weaker adjacent crusts in which deformation is strongly partitioned. The positive feedback loop between strain, retrogression, and weakening insures that deformation remains localized into retrogressed domains, isolating and protecting garnet-pyroxene-bearing pods that remain largely immune to deformation.

CONCLUSIONS

In this study, we have explored through 2-D thermomechanical modeling how the interplay between partial melting, the formation of garnet-pyroxene high-grade rocks, and strain rate–dependent retrogression could explain the long-term preservation of deep crustal roots in stable continents. Though 2-D experiments are sufficient to illustrate how strain rate, retrogression, and weakening can explain the preservation of thick roots, future work involving 3-D experiments will allow investigation of triclinic boundary conditions. Our experiments show that following the formation of high-grade rocks in deep orogenic crusts, extension is partitioned into regions where strain, retrogression, and weakening are coupled into a positive feedback loop. This results in the preservation of thick, dense, and strong garnet-pyroxene-rich pods, separated by retrogressed and attenuated pinched regions. The strong high-grade pods form crustal-scale boudins that are able to survive through the orogenic relaxation phase and over a duration of >100 m.y. As a result, the equilibrated orogenic crust preserves deep crustal roots similar to those documented in all stable continents. These results are first steps toward understanding of the feedback between metamorphic reactions and deformation. In the future, 3-D models involving porous flow and surface processes will allow a more detailed understanding of these systems.

ACKNOWLEDGMENTS

We acknowledge funding from the European Union's Horizon 2020 research and innovation program under grant agreement 793978. This research was undertaken with the assistance of resources from the National Computational Infrastructure (NCI), through the National Computational Merit Allocation Scheme supported by the Australian Government; the Pawsey Supercomputing Centre (Perth, Australia) with funding from the Australian Government and the Government of Western Australia, and support from the Australian Research Council through the Industrial Transformation Research Hub grant ARC-IH130200012. We thank Julian Giordani and Romain Beucher for their expert support with *Underworld* (https://underworld2.readthedocs.io/). We thank Chris Clark for editorial handling, as well as Gregory Dumond and two anonymous reviewers for their constructive reviews.

REFERENCES CITED

An, M., Wiens, D.A., Yue, Z., Mei, F., Nyblade, A.A., Kanao, M., Li, Y., Maggi, A., and Lévêque, J.-J., 2015, *S*-velocity model and inferred Moho topography beneath the Antarctic Plate from Rayleigh waves: Journal of Geophysical Research: Solid Earth, v. 120, p. 359–383, https://doi.org/10.1002/2014JB011332.

Artemieva, I.M., and Thybo, H., 2013, EUNAseis: A seismic model for Moho and crustal structure in Europe, Greenland, and the North Atlantic region: Tectonophysics, v. 609, p. 97–153, https://doi.org/10.1016/j.tecto.2013.08.004.

Beaumont, C., Jamieson, R.A., Nguyen, M.H., and Lee, B., 2001, Himalayan tectonics explained by extrusion of a low-viscosity crustal channel coupled to focused surface denudation: Nature, v. 414, p. 738–742, https://doi.org/10.1038/414738a.

Beucher, R., et al., 2019, UWGeodynamics: A teaching and research tool for numerical geodynamic modelling: Journal of Open Source Software, v. 4, 1136, https://doi.org/10.21105/joss.01136.

Boutonnet, E., Leloup, P.H., Sassier, C., Gardien, V., and Ricard, Y., 2013, Ductile strain rate measurements document long-term strain localization in the continental crust: Geology, v. 41, p. 819–822, https://doi.org/10.1130/G33723.1.

Cenki-Tok, B., Berger, A., and Gueydan, F., 2016, Formation and preservation of biotite-rich microdomains in high-temperature rocks from the Antananarivo Block, Madagascar: International Journal of Earth Sciences, v. 105, p. 1471–1483, https://doi.org/10.1007/s00531-015-1265-0.

Christensen, N.I., and Mooney, W.D., 1995, Seismic velocity structure and composition of the continental crust: A global view: Journal of Geophysical Research, v. 100, p. 9761–9788, https://doi.org/10.1029/95JB00259.

Clark, M.K., and Royden, L.H., 2000, Topographic ooze: Building the eastern margin of Tibet by lower crustal flow: Geology, v. 28, p. 703–706, https://doi.org/10.1130/0091-7613(2000)28<703:TOBTEM>2.0.CO;2.

Cook, F.A., White, D.J., Jones, A.G., Eaton, D.W.S., Hall, J., and Clowes, R.M., 2010, How the crust meets the mantle: Lithoprobe perspectives on the Mohorovic discontinuity and crust–mantle transition: Canadian Journal of Earth Sciences, v. 47, p. 315–351, https://doi.org/10.1139/E09-076.

Das, R., Ashish, and Saha, G.K., 2019, Crust and shallow mantle structure of south India by inverting interpolated receiver function with surface wave dispersion: Journal of

Asian Earth Sciences, v. 176, p. 157–167, https://doi.org/10.1016/j.jseaes.2019.02.011.

Ebbing, J., Hass, P., Ferraccioli, F., Pappa, F., Szwillus, W., and Bouman, J., 2018, Earth tectonics as seen by GOCE—Enhanced satellite gravity gradient imaging: Scientific Reports, v. 8, https://doi.org/10.1038/s41598-018-34733-9.

Fagereng, Å., and Biggs, J., 2019, New perspectives on 'geological strain rates' calculated from both naturally deformed and actively deforming rocks: Journal of Structural Geology, v. 125, p. 100–110, https://doi.org/10.1016/j.jsg.2018.10.004.

Fischer, K.M., 2002, Waning buoyancy in the crustal roots of old mountains: Nature, v. 417, p. 933–936, https://doi.org/10.1038/nature00855.

Funck, T., and Louden, K.E., 1999, Wide-angle seismic transect across the Torngat Orogen, northern Labrador: Evidence for a Proterozoic crustal root: Journal of Geophysical Research, v. 104, p. 7463–7480, https://doi.org/10.1029/1999JB900010.

Jackson, J.A., Austrheim, H., McKenzie, D., and Priestley, K., 2004, Metastability, mechanical strength, and the support of mountain belts: Geology, v. 32, p. 625–628, https://doi.org/10.1130/G20397.1.

Kennett, B.L.N., Salmon, M., Saygin, E. and the AusMoho Working Group, 2011, AusMoho: The variation of Moho depth in Australia: Geophysical Journal International, v. 187, p. 946–958, https://doi.org/10.1111/j.1365-246X.2011.05194.x.

Korchinski, M., Rey, P.F., Mondy, L., Teyssier, C., and Whitney, D.L., 2018, Numerical investigation of deep-crust behavior under lithospheric extension: Tectonophysics, v. 726, p. 137–146, https://doi.org/10.1016/j.tecto.2017.12.029.

Moresi, L., Quenette, S., Lemiale, V., Meriaux, C., Appelbe, B., and Mühlhaus, H.-B., 2007, Computational approaches to studying non-linear dynamics of the crust and mantle: Physics of the Earth and Planetary Interiors, v. 163, p. 69–82, https://doi.org/10.1016/j.pepi.2007.06.009.

Nábělek, J., Hetényi, G., Vergne, J., Sapkota, S., Kafle, B., Jiang, M., Su, H.P., Chen, J., Huang, B.S., and the Hi-CLIMB Team, 2009, Underplating in the Himalaya-Tibet collision zone revealed by the Hi-CLIMB Experiment: Science, v. 325, p. 1371–1374, https://doi.org/10.1126/science.1167719.

O'Reilly, S.Y., and Griffin, W.L., 2013, Moho vs crust-mantle boundary: Evolution of an idea: Tectonophysics, v. 609, p. 535–546, https://doi.org/10.1016/j.tecto.2012.12.031.

Philpotts, A.R., and Ague, J.J., 2009, Principles of Igneous and Metamorphic Petrology: Cambridge, UK, Cambridge University Press, 667 p., https://doi.org/10.1017/CBO9780511813429.

Prodehl, C., Kennett, B., Artemieva, I.M., and Thybo, H., 2013, 100 years of seismic research on the Moho: Tectonophysics, v. 609, p. 9–44, https://doi.org/10.1016/j.tecto.2013.05.036.

Reddy, P.R., and Vijaya Rao, V., 2013, Seismic images of the continental Moho of the Indian shield: Tectonophysics, v. 609, p. 217–233, https://doi.org/10.1016/j.tecto.2012.11.022.

Rey, P.F., and Müller, R.D., 2010, Fragmentation of active continental plate margins owing to the buoyancy of the mantle wedge: Nature Geoscience, v. 3, p. 257–261, https://doi.org/10.1038/ngeo825.

Rey, P.F., Teyssier, C., and Whitney, D.L., 2009, Extension rates, crustal melting, and core complex dynamics: Geology, v. 37, p. 391–394, https://doi.org/10.1130/G25460A.1.

Rey, P.F., Teyssier, C., and Whitney, D.L., 2010, The limit of channel flow in orogenic plateaux: Lithosphere, v. 2, p. 328–332, https://doi.org/10.1130/L114.1.

Rey, P.F., Teyssier, C., Kruckenberg, S.C., and Whitney, D.L., 2011, Viscous collision in channel explains double domes in metamorphic core complexes: Geology, v. 39, p. 387–390, https://doi.org/10.1130/G31587.1.

Rey, P.F., Mondy, L., Duclaux, G., Teyssier, C., Whitney, D.L., Bocher, M., and Prigent, C., 2017, The origin of contractional structures in extensional gneiss domes: Geology, v. 45, p. 263–266, https://doi.org/10.1130/G38595.1.

Salmon, M., Kennett, B.L.N., Stern, T., and Aitken, A.R.A., 2012, The Moho in Australia and New Zealand: Tectonophysics, v. 609, p. 288–298, https://doi.org/10.1016/j.tecto.2012.07.009.

Sassier, C., Leloup, P.H., Rubatto, D., Galland, O., Yue, Y., and Lin, D., 2009, Direct measurement of strain rates in ductile shear zones: A new method based on syntectonic dikes: Journal of Geophysical Research, v. 114, B01406, https://doi.org/10.1029/2008JB005597.

Studinger, M., Bell, R.E., Buck, W.G., Karner, G.D., and Blankenship, D.D., 2004, Sub-ice geology inland of the Transantarctic Mountains in light of new aerogeophysical data: Earth and Planetary Science Letters, v. 220, p. 391–408, https://doi.org/10.1016/S0012-821X(04)00066-4.

Szwillus, W., Afonso, J.C., Ebbing, J., and Mooney, W.D., 2019, Global crustal thickness and velocity structure from geostatistical analysis of seismic data: Journal of Geophysical Research: Solid Earth, v. 124, p. 1626–1652, https://doi.org/10.1029/2018JB016593.

Thybo, H., and Artemieva, I.M., 2013, Moho and magmatic underplating in continental lithosphere: Tectonophysics, v. 609, p. 605–619, https://doi.org/10.1016/j.tecto.2013.05.032.

White, R.W., Powell, R., and Holland, T.J.B., 2001, Calculation of partial melting equilibria in the system Na_2O–CaO–K_2O– FeO–MgO–Al_2O_3–SiO_2–H_2O (NCKFMASH): Journal of Metamorphic Geology, v. 19, p. 139–153, https://doi.org/10.1046/j.0263-4929.2000.00303.x.

Williams, M.L., Dumond, G., Mahan, K., Regan, S., and Holland, M., 2014, Garnet-forming reactions in felsic orthogneiss: Implications for densification and strengthening of the lower continental crust: Earth and Planetary Science Letters, v. 405, p. 207–219, https://doi.org/10.1016/j.epsl.2014.08.030.

FIGURE CAPTIONS

Figure 1. (A) Crustal thickness histogram for world shields extracted from CRUST 5.1 model (modified from https://earthquake.usgs.gov/data/crust/crust.php). (B) Interpolated compressional-wave velocities across the Torngat orogen, northeastern Canada (modified from Funck and Louden, 1999). (C) Interpolated Moho surfaces for Australia constructed by interpolating weighted averages for each 0.5° × 0.5° pixel (modified from Kennett et al., 2011).

Figure 2. Model geometry and initial conditions, as well as geotherm, viscosity, and density profiles. Weak prismatic region dipping 45° simulates detachment fault in upper crust. Circles pattern superimposed on continental crust represents finite-strain ellipses.

Figure 3. Fast-velocity modeling results (1.8 cm yr^{-1} extension speed) at average strain rate of 3×10^{-15} s^{-1} and 25% extension. Colors are the same as in Figure 2. (Model A) Only partial melting is allowed (garnet-pyroxene isograde and retrogression into amphibolite are removed). (Model B) Partial melting, crystallization of garnet-pyroxene assemblages, and retrogression are allowed. Temperature for transformation of continental crust into garnet-pyroxene-rich rocks is 777 °C (see text for explanation). Reference temperatures for solidus of continental crust and garnet-pyroxene-rich crust are 650 °C and 790 °C, respectively. (Model C) Same as model B but temperature for continental crust solidus is increased to 720 °C. (Model D) Zoom on model B illustrating velocity field (black arrows) when boundary condition mimicking extension is removed (after 2 m.y. of gravity forces operating), showing that partially molten crust flows while garnet-pyroxene-rich rocks do not.

Figure 1

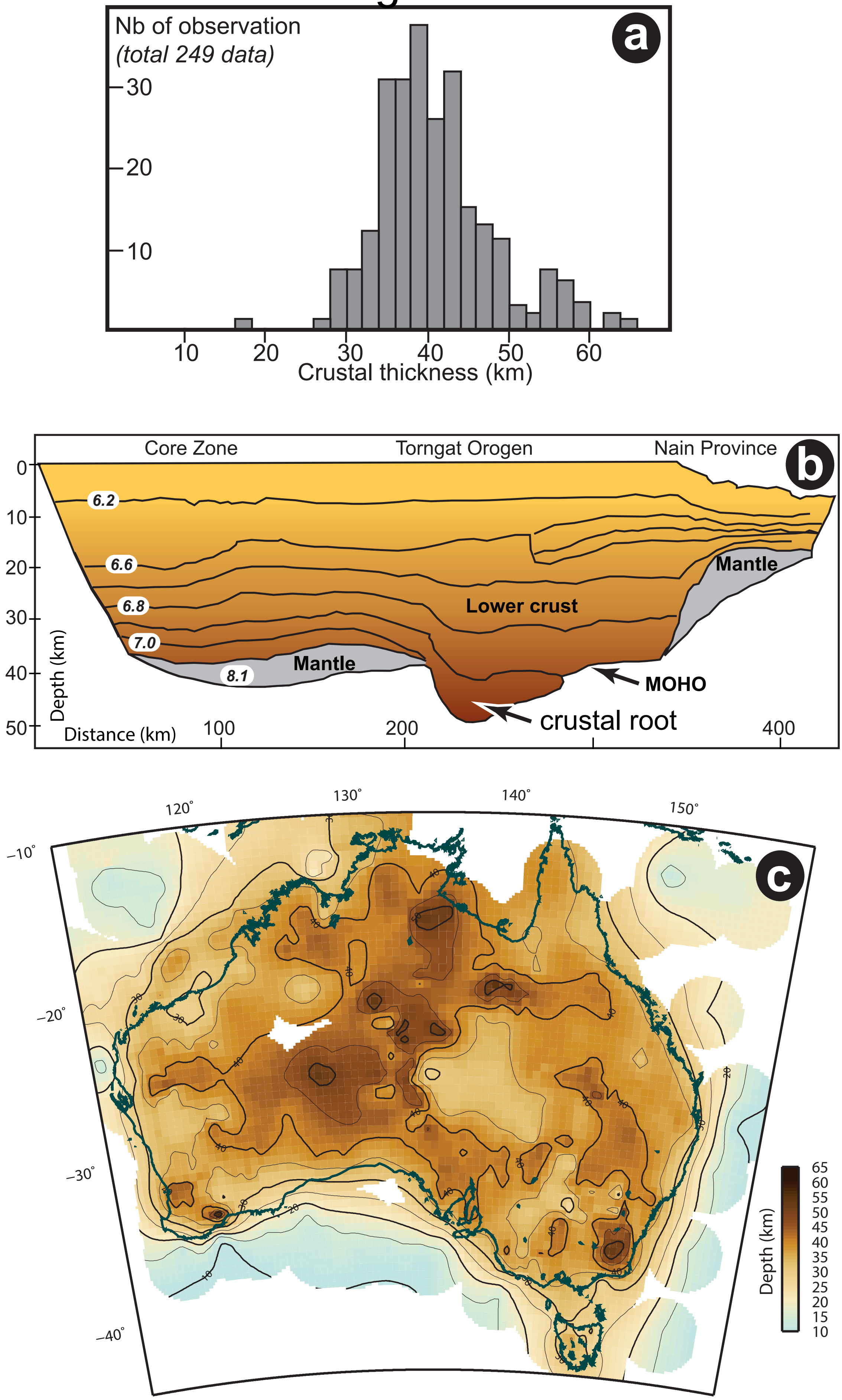

Figure 1

Figure 2

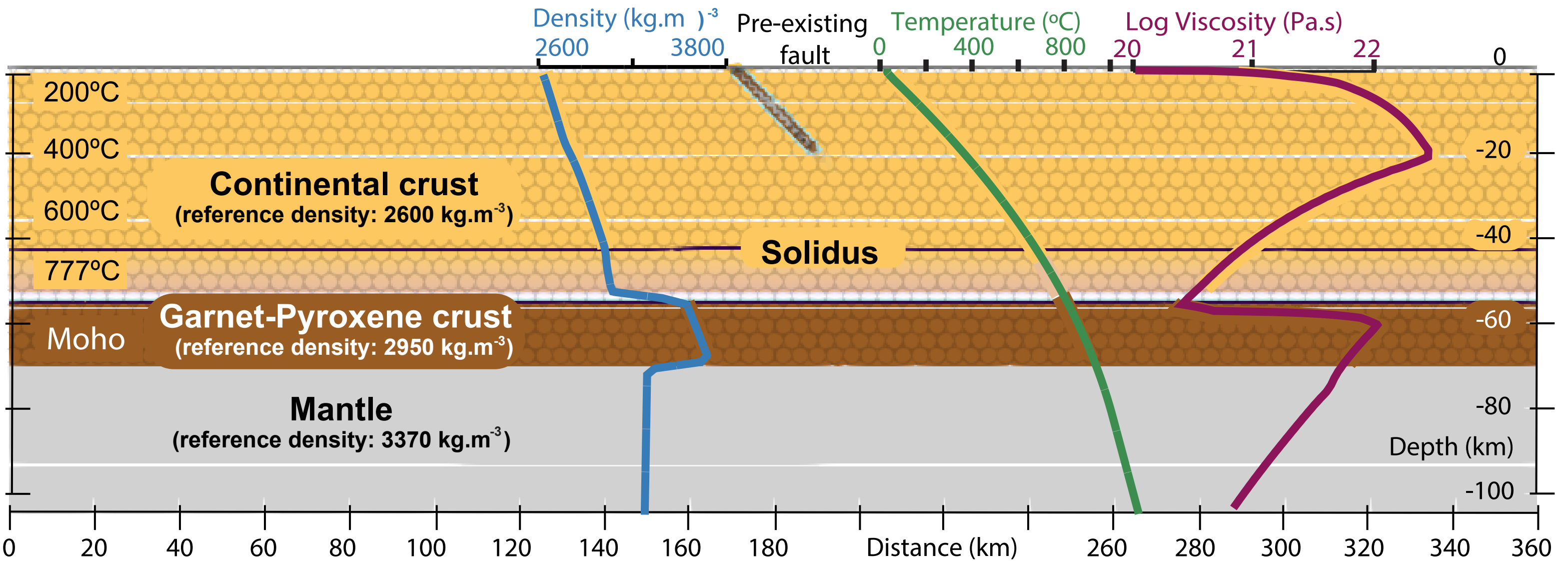

Figure 2

Figure 3

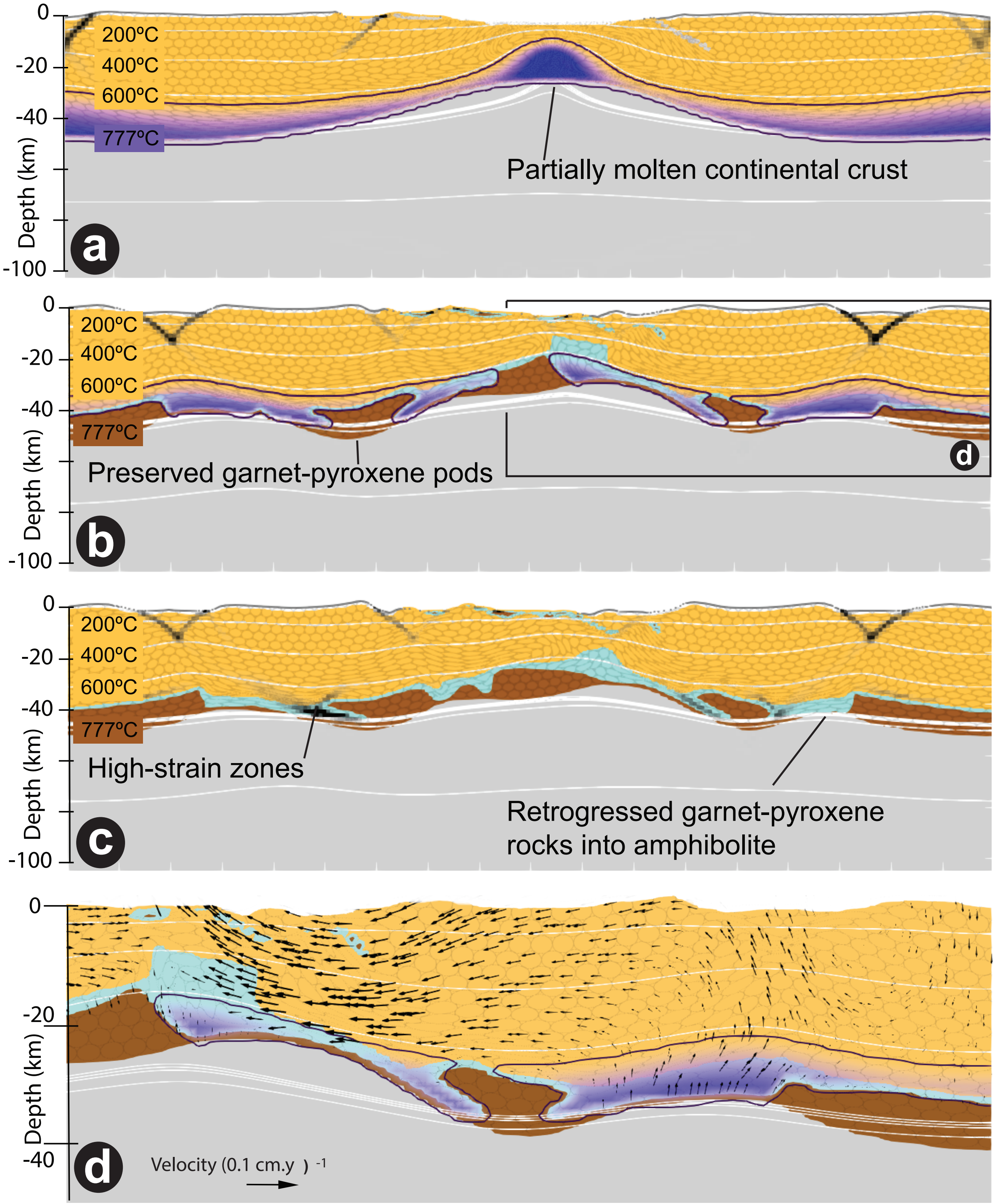

Figure 3

Strain and retrogression partitioning explain long-term stability of crustal roots in stable continents

Bénédicte Cenki-Tok [1,2], P.F. Rey[2] and D. Arcay[1]

TABLE DR1. THERMAL AND MECHANICAL PARAMETERS

Parameter	Continental Crust	Retrogressed Amphibolites	Garnet-Pyroxene CC	Upper Mantle	Fault
Reference temperature (K)	293	293			
Dislocation creep viscous rheology	Wet quartzite[a]	Wet quartzite[a]	Dry Maryland Diabase [b]	Wet dunite [c]	0.1 *Wet quartzite[a]
Reference density ($kg \cdot m^{-3}$)	2600	2600	2950	3370	2600
Thermal expansivity (K-1)	-1.00E-04	-1.00E-04	-1.00E-04	2.80E-05	-1.00E-04
Compressibility (Pa^{-1})	8.00E-11	8.00E-11	-	-	8.00E-11
Heat capacity ($J\ K^{-1}\ kg^{-1}$)	1000	1000	1000	1000	1000
Thermal diffusivity ($m^2\ s^{-1}$)	9E-07	9E-07	9E-07	9E-07	9E-07
Latent heat of fusion ($kJ\ kg^{-1}\ K^{-1}$)	250	250	250	-	250
Radiogenic heat production ($W\ m^{-3}$)[d]	5.00E-07	5.00E-07	5.00E-07	-	5.00E-07
Melt fraction density change[e]	0.13	0.13	-	-	0.13
Solidus term 1 (K)	923	923	1063	-	923
Solidus term 2 ($K\ Pa^{-1}$)	-1.20E-07	-1.20E-07	-1.20E-07	-	-1.20E-07
Solidus term 3 ($K\ Pa^{-2}$)	1.20E-16	1.20E-16	1.20E-16	-	1.20E-16
Liquidus term 1 (K)	1423	1423	1563	-	1423
Liquidus term 2 ($K\ Pa^{-1}$)	-1.20E-07	-1.20E-07	-1.20E-07	-	-1.20E-07
Liquidus term 3 ($K\ Pa^{-2}$)	1.60E-16	1.60E-16	1.60E-16	-	1.60E-16
Friction coefficient	0.44	0.44	0.44	0.44	0.44
Softened friction coefficient	0.088	0.088	0.088	0.088	0.088
Cohesion (MPa)	15	15	15	15	1.5
Softened cohesion (MPa)	3	3	3	3	0.3
Pre-exponential factor ($MPa^{-n}\ s^{-1}$)	5.00E-06	5.00E-06	5.05E-22	70000	5.00E-06
Stress exponent (n)	3	3	4.7	3	3
Activation energy ($kJ\ mol^{-1}$)	190	190	485	520	190
Activation volume ($m^3\ mol^{-1}$)	0	0	0	0	0
Water fugacity	0	0	0	0	0
Water fugacity exponent[f]	0	0	0	0	0
Melt viscous softening factor	1.00E-03	1.00E-03			1.00E-03
Softening melt fraction interval	0.2-0.3	0.2-0.3			0.2-0.3

Additional parameters:
Model Size: 360 km length (241 nodes, constant spacing) - 120 km thick (81 nodes, constant spacing) i.e. 15 km air-like material, 70 km crust, 35 km upper mantle. The marker density is uniform (60 per grid cell).
A weak prismatic region dipping 45 °C simulates a detachment in the upper crust
Basal heat flow is set at 0.015 $W.m^{-2}$
Velocities tested: 1.8 $cm.y^{-1}$ (fast) or 0.18 $cm.y^{-1}$ (slow) and Isostasy is activated
Prograde amphibolite to garnet-pyroxene rock phase change set at 1050 K
Retrograde garnet-pyroxene rock to amphibolite phase change set at 1050 K and 10-^{14} s^{-1} strain rate
Moho temperature at the start of the model is 883 °C
Solidus and liquidus are defined by a polynomial function of pressure (P):
$T_s = a_0 + a_1 \times P + a_2 \times P^2$, $T_l = b_0 + b_1 \times P + b_2 \times P^2$
The density of the continental crust changes according to T and P:
$\rho = \rho_0 * (1 + (\beta * \Delta P) - (\alpha * \Delta T))$
Note that the presence of melt has an impact on density.
The maximum melt fraction is 30%.

References:
a Parameters were derived from Brace and Kohlstedt (1980)
b Parameters were derived from Mackwell et al (1998)
c Parameters were derived from Brace and Kohlstedt (1980)
d Parameters were derived from Hasterok and Chapman (2011)
e Melt and other parameters were derived from Rey and Muller (2010)
f A zero value denotes that this effect on the viscous flow law is incorporated into the pre-exponential factor

DR Figure1: Slow modeling results (0.18 cm.y^{-1} extension speed) at an average strain rate of 3e-16 s^{-1} and 25 % extension. Colors are the same as in Fig. 2. Conditions for a, b and c models are the same as in Fig. 3.

DR Figure2: Fast modeling results (1.8 cm.y^{-1} extension speed) at an average strain rate of 3e-15 s^{-1} and 25 % extension. Colors are the same as in Fig 3. Variations of model shown on Figure 3b but a. only the prograde phase change is allowed. Retrogression does not occur, and the crust, including the garnet-pyroxene layer, thins homogeneously. b. The strain rate threshold for retrogression has been set to 10^{-13} s^{-1}. Retrogression does not occur, and the crust, including the garnet-pyroxene layer, thins homogeneously. c. The strain rate threshold for retrogression has been set to 10^{-15} s^{-1}, large portions of retrogressed and partially molten crust are exhumed in the center of the model whereas the garnet-pyroxene layer is preserved locally but strongly thinned.

REFERENCES CITED:

Brace, W.F., and Kohlstedt, D.L., 1980, Limits on lithospheric stress imposed by laboratory experiments: Journal of Geophysical Research, v. 85, p. 6248-6252.

Hasterok, D., Chapman, D., 2011. Heat production and geotherms for the continental lithosphere. Earth Planet. Sci. Lett. 307 (1), 5970.

Mackwell, S. J., Zimmerman, M. E., & Kohlstedt, D. L. (1998). High-temperature deformation of dry diabase with application to tectonics on Venus. Journal of Geophysical Research: Solid Earth, 103(B1), 975-984.

Rey, P.F., Muller, R.D., 2010. Fragmentation of active continental plate margins owing to the buoyancy of the mantle wedge. Nat. Geosci. 3 (4), 257–261.

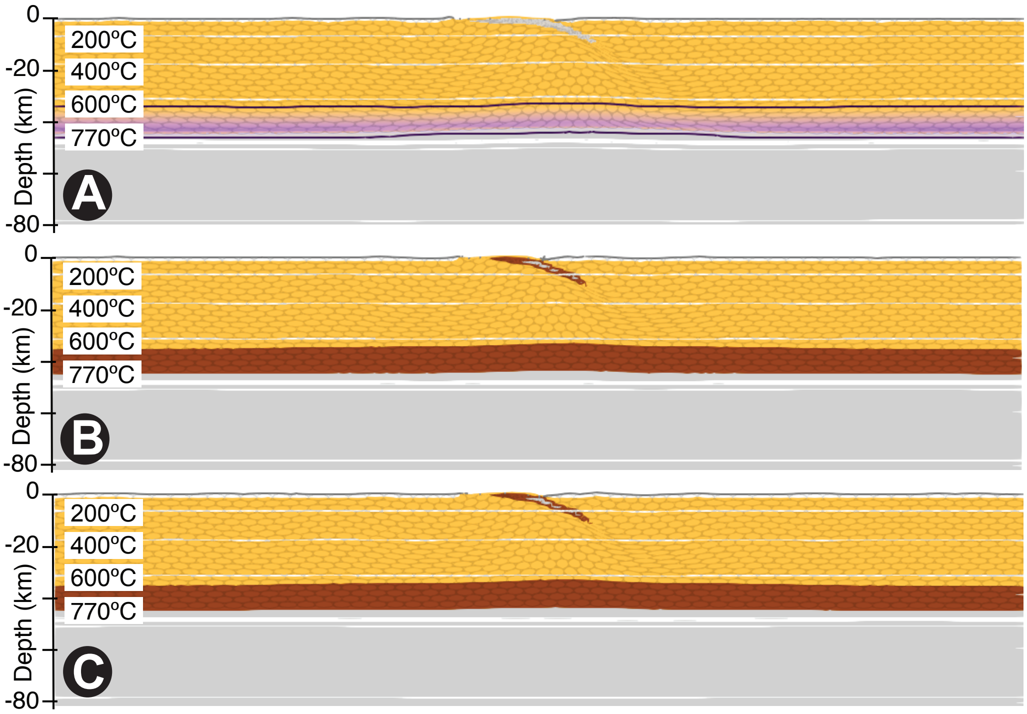

Supplementary Data Figure1

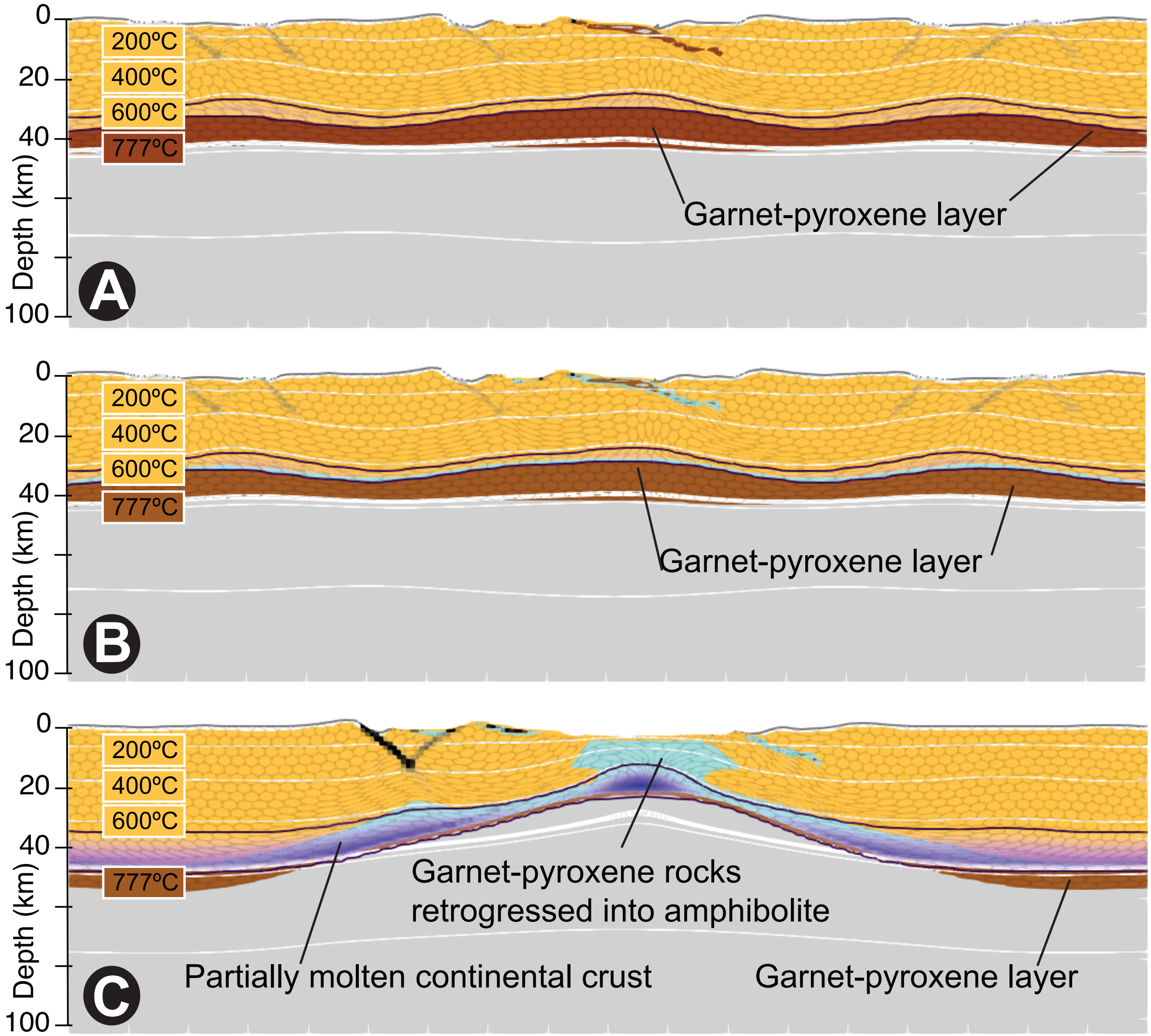

Supplementary Data Figure2